THE STRUCTURE AND BRIEF REVIEW ON $Ba(NO_3)_2$, KNO_3 AND DISPERSED SOLID ELECTROLYTES

I STRUCTURE OF $Ba(NO_3)_2$ AND KNO_3

I.1 $Ba(NO_3)_2$

Barium nitrate is an isomorphous crystal with other nitrates such as Ca, Sr & Pb forming a group. It has a cubic structure with the space group Pa_3 and it belong to T_h^6 class [1]. In the cubic system the symbol 'T' is used for tetrahedral symmetry group with four triad and three diad axes.

CaF_2 in its naturally occurring form is called the 'fluorite' and the compounds which crystallize in this form are called fluorites. The Nitrates of Ca, Ba, Sr and Pb are isomorphous and have fluorite type structure [1]. The two- and three-dimensional structure of fluorite RX_2 lattice is shown in figure I.1. Eight comparable nearest neighbour ions of species X surround each ion of species R in a compound RX2, forming the corners of a cube with R at its centre. A tetrahedron of four comparable R ions surrounds each ion of species X. At a more fundamental level, the structure consists of a space lattice of symmetry Oh5 and a face-centered cubic translational group.

An interpretation of the structure is given in terms of a primitive cube with side "a." It consists of three face-centered cubic lattices that are interpenetrating. The first is a species R lattice whose origin is at (0,0,0) and whose primitive translational vectors are in the cube of side a and are (0, 1/2, 1/2); (1/2, 0, 1/2); and (1/2, 1/2, 0). The X species have beginnings at (1/4, 1/4, 1/4) and (3/4, 3/4, 3/4a) on two additional lattices that have comparable translational vectors. Located at the core of a cube containing eight X ions, the R ion site exhibits Oh symmetry.

It is clear that the various atom or ion species are in intimate contact with one another because to the fluorite structure. Moreover, close interaction between the ions of species X is inhibited if the ions of species R are big enough. In the event that the constituent species are viewed as hard spheres

with radii of r(R) and r(X), contact between the R and X ions happens when the radii meet the requirement 4.45 > r(R), excluding both X-X and R-R [2] contact $4.45 \geq r(R) / r(X) \geq 0.73$.

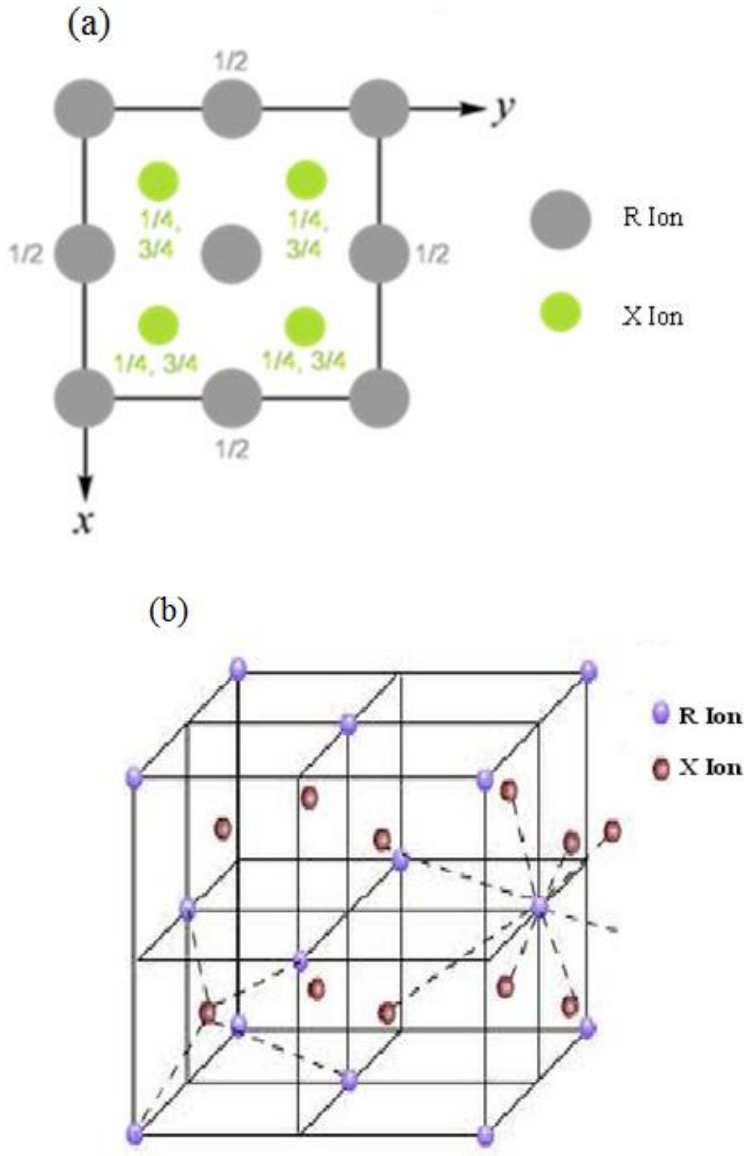

Fig.1.1 The Fluorite structure of the (a) two dimensional and (b) three dimensional RX_2 Lattice.

Strongly ionic compounds with formula RX2 that contain big ions of type R are likely to favour the fluorite structure due to the potential of close contact between different ions. Actually, the R ions are typically somewhat little, and there are a number of series of compounds where one ion

can cross the other limiting value and make contact with the X ions. For instance, one observes that the iodides have orthorhombic or sheet-like structures, but the halides of cadmium or barium have a fluorite lattice structure for the smaller halide (X) ions.

The materials found to possess the fluorite structure have been divided by Wyckoff [2] into four main classes:

i. The halides of the larger divalent cations (all but two are in fact fluorides) e.g., CaF_2, SrF_2, BaF_2, CdF_2, PbF_2, $SrCl_2$, $BaCl_2$.

ii. The oxides of certain large quadrivalent cations.
e.g., ZrO_2, CeO_2, ThO_2, and UO_2.

iii The oxides and other chalcogenides of alkali and other univalent cations.
e.g., K_2S, Na_2S and Li_2Se.

iv Miscellaneous intermetallic compounds and the oxy fluorides and hydrides of rare earth elements.

The compounds in category (i) of the aforementioned classification share structural similarities with the nitrates of Ca, Sr, Ba, and Pb. The F-ion of the CaF2 structure is replaced in Ba(NO3)2 by an anion made up of nitrogen in the middle and oxygen filling the corners of an equilateral triangle. Whether all four of the atoms are coplanar is a matter of debate. There have been two theories put forth. Four molecules make comprise the unit cell in the previous opinion put up by Vegard [3], wherein Th6 space group is allocated to them. Since all three anions in this instance are coplanar with the nitrogen at the center, there is an inversion center and all three NO3 groups are comparable to one another.

T4 space group is assigned in Birnstock's [4] second hypothesis, which is based on neutron scattering observations. In this instance, two distinct nitrate groups can be identified, and the center of inversion is absent. According to this idea, the oxygens and nitrogen are no longer coplanar; instead, the nitrogen atom is believed to be displaced off the oxygens' plane, resulting in a pyramidal structure. Bon et al [5] have carried out the studies of infrared reflection spectra on the single crystals of these isomorphous compounds. The results were discussed and they concluded that the T^4 structure is more appropriate on the basis of their studies.

Srinivasan [6] has determined that the link between the metal ion and the nitrate ion is mainly ionic after considering a number of characteristics of these crystals, including the melting points, solubility, thermal expansion, elastic constants, intensity of the Raman lines, and magneto-optic anomaly. Due to coulomb attraction, ionic crystals have an extremely high binding force, which raises their melting point. Poor electrical and thermal conductivity is to be expected as there aren't ideal free electrons. Ionic conductivity can be produced as the temperature gets close to the melting point because the ions become more mobile at that moment. Good optical transparency across a significant portion of the electro-magnetic spectrum is also implied by the absence of free electrons. Until the photon energy reaches around 6eV, or the far ultraviolet, it cannot drive an electron out of one of the filled ionic shells and cause optical absorption.

I.2 KNO_3

Potassium nitrate was discovered in 1958 as a ferroelectric material by Sawada et al [7]. Since then KNO_3 has been investigated by many researchers from the ferroelectric, dielectric, and structural view point [8]. Since the late 1960s, it has been established that, depending on external state variables, KNO3 occurs in one of multiple crystallographic phases. Ferroelectric phase III is the only phase that is known to exist at high temperatures when cooling from higher temperatures. This

ferroelectric phase III would be of technological interest if it can be stabilized at room temperature. KNO_3 has been found to possess aragonite structure known as phase II by many researchers at room temperature.

The molecular structure of KNO_3 has been investigated for the first time by electron diffraction by patrov et al [9]. Assuming a bidentate configuration of the KNO3 molecule with C2v symmetry and D3h local symmetry of the NO3 fragment, the first stage of structural analysis was carried out. Table I illustrates the range of phases in which KNO3 has been discovered to occur. The crystal structure changes from orthorhombic (phase-II) to rhombohedral (phase-I) during heating, and upon cooling, phase-I becomes ferroelectric phase-III at approximately 124ºC, and phase-III becomes phase-II at approximately 110ºC [10–13].

TABLE-I The different phases of KNO_3

Phase of KNO_3	**Temperature (ºC)**	**Unit –cell data (Å)**			**Crystal structure**
		a	B	C	
Phase II	130	5.414	9.164	6.431	Orthorhombic
Phase I	124	5.423	5.423	9.638	Rhombohedral
Phase III	110	5.430	5.430	9.095	Rhombohedral

The crystal structure and related parameters of different phases of KNO_3 are shown in figure I.2. The phase transitions also accompany the variation in the unit cell's volume. The relative volume changes of KNO_3 unit cell associated with the phase II → phase I, phase I → phase III, phase III → phase II transitions are +0.27, -5.375, and -3.56 %, respectively [14].

The phase II → phase I transition increases the overall density of the loosely packed structure. However, the decrease in the volume during the phase I → phase III transition allows the structure to

increase the packing density. This packing places the KNO_3 under an effective stress, which is known to affect the phase transition temperatures. This effective applied stress enhances the sintering of the KNO_3 particles [15].

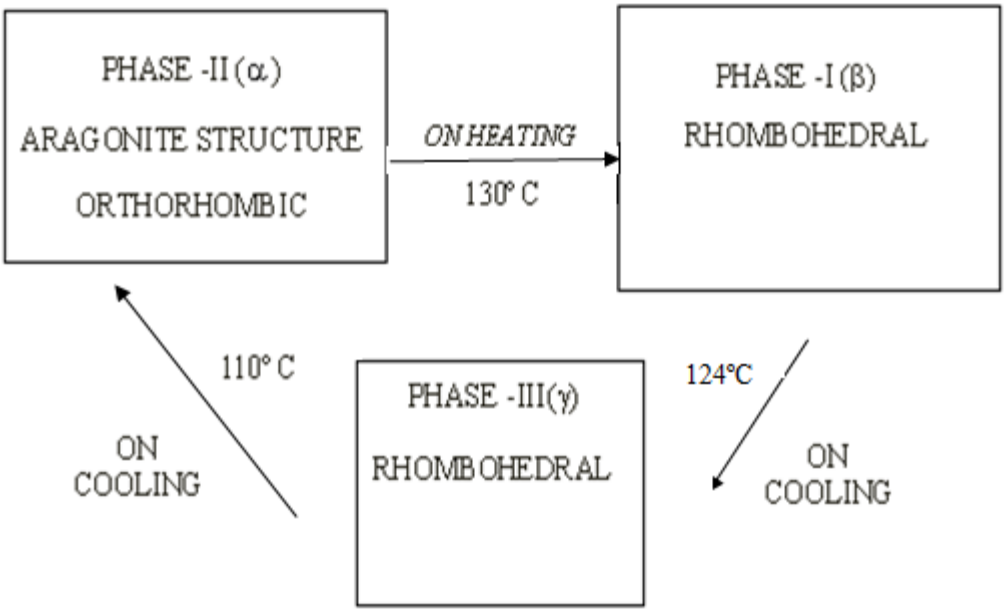

Fig.1.2 Crystal structure changes when KNO_3 was passed through the heating and cooling cycles.

The crystal structures of the phase I and phase II are non-polar, but that of the phase III is polar. The corresponding crystal structures of aragonite and γ-phase of KNO_3 as seen in the figures I.3(a) and 3.3(b) respectively. The stable phase of KNO3 is aragonite at room temperature and γ-phase is the rhombohedral unit cell in the ferroelectric phase III which contains one molecule of KNO_3 and K^+ ions occupy its corners whereas NO_3^- ion lies near its body center. The NO_3 group forms a regular triangle with the N atom at its center. The plane of the NO_3 group is perpendicular to the c-axis and it does not exist exactly at the body center [15]. One of the several materials suggested [16] as a standard reference material in thermal analysis is potassium nitrate. The alkali nitrate crystals are

dielectric ones with the variation in both the conductivity and the crystal structures at their phase transitions.

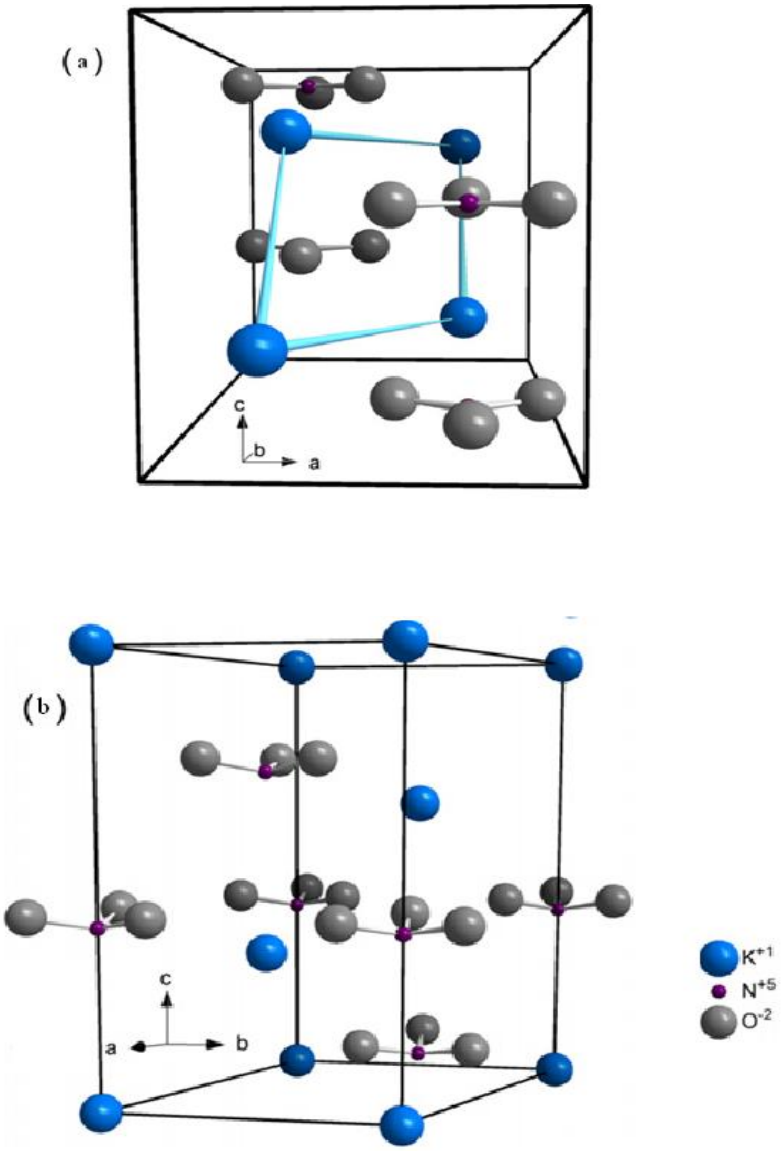

Fig 1.3 Crystal structure views of KNO_3 a) aragonite, (b) γ -phase.

II A BRIEF REVIEW ON DISPERSED SOLID ELECTROLYTES

Mixed crystals' many uses sparked a great deal of interest and curiosity, which led to in-depth research. The study of transport processes in ionic crystals has received a lot of attention over the past

several years. Conductivity investigations, among other transport processes, offer important insights into the condition of point defects in ionic crystals. The migration of positive ion vacancies is responsible for the ionic conductivity of these crystals at temperatures that are not particularly close to the melting point [17].

Ionic conductivity measurements as a function of temperature have been done by a number of researchers. The most of the work is done on alkali halide crystals doped with anion as well as cation impurities [18-20], since they are easily obtainable ionic compounds of relatively simple crystal structure. However, the work on mixed crystals is very limited. Lehfeldt[21], and Phipps and Patridge [22] investigated conductivities of several alkali halides, including KBr and KCl, while Kelting and Witt [23] established the effect of divalent impurities on conductivity. Ambrose and Walace's [24] ionic conductivity studies on KCl-KBr mixed crystals revealed that the conductivity of the mixed crystals never deviates significantly from the conductivity range set by the pure end components, suggesting that the population of vacancies in mixed crystals is identical to that of pure end crystals. Nonetheless, the conductivity investigations of Schultze [25], Annenkov et al. [26], Arends et al. [27] and Zayadowskaya et al. [28] showed that the vacancy concentration in mixed crystals is higher than in the pure end components.

Ionic conductivity studies in KCl-KI mixed crystals have been done by U.V. Subbarao and V. Haribabu [29]. Ionic conductivity studies in KCl–NaCl mixed crystals were done by P.Veerasham et al [30]. Anomalous ionic conduction AgBr-AgI mixed crystals and multiphase systems have been studied by K.Shahi et al [31]. Growth and study of mixed crystals of Ca-Cd iodate were studied by S.L Garud et al [32]. Growth and characterization of mixed crystals of NaBr-KBr were studied by C.M. Padma et al [33]. These investigations' findings suggest that the structure of faults in mixed crystals differs from that of their pure positions. The local pressures caused by the disparity in atomic sizes between mixed crystals alter the lattice's characteristics and its lattice parameters [34]. Additionally, optical, opto-electronic, and electronic devices found use for mixed alkali halides.

Very little research has been done on alkaline and alkali earth nitrates. J. Kudrnovsky et al. conducted research on the electronic structure of compounds of the fluorite type and mixed crystals [35]. Wen-Ming Chien et al. [36] investigated X-ray diffractometry investigations and lattice parameter computation on KNO3-NH4NO3 solid solution. In recent times, there has been an increased focus on the superionic conductivity of fluorite-type compounds and their derived mixed crystals. A review of the literature reveals that, in contrast to alkali nitrates generally, no research has been done on the dc ionic conductivity of mixed crystals made up of alkaline earth nitrates. Moreover, no such conductivity studies have been done specifically for mixed crystals made up of Ba(NO3)2 and KNO3.

The development of dispersed solid electrolytes can be linked to the observations made during the beginning of this century [37] that the conductivity of two-phase mixtures may exceed the conductivities of pure constituents. Wagner [38] and Crosbie [39] studied the conductivity behavior of semiconductors, with small inclusions of another non-conducting phase and found that the conductivities exceeded those of pure constituents. Recently, this approach has been extended to solid electrolytes in order to bring about enhancements in their ionic conductivities. Most of the work reported in the literature has been done with the dispersion of insulators such as Al_2O_3, SiO_2, fly ash, ZrO_2 etc., in ionic conductors. Among these in the present work the alumina with particle size (1 µm, 0.3µm, 0.06µm), SiO_2(20nm), CeO_2(15nm) were used in the preparation of the dispersed solid electrolyte networks.

In the following sections analysis of the work already done in the form of dispersed solid electrolyte systems is presented exhaustively.

II.1 LITHIUM HALIDES

Liang [40] is almost the founder of studies on dispersed systems who first reported his results in Anhydrous LiI dispersed with Al_2O_3. As per his observations there was a maximum in conductivity of about 10^{-5} S/Cm at 25^0C at around 40 mole percent of Al_2O_3. It was found that the electronic conductivity of these systems was insignificant compared to the ionic conductivity. The conduction mechanism was attributed to the cation vacancies which are the species responsible for conduction in pure LiI. It was also confirmed by X-Ray diffractograms (XRD) that there was no indication of formation of any solid solution. The discharge and storage characteristics indicated that the system functioned as a practical, low rate solid-state battery system [41]. However, the conductivity studies [42] on LiI.H_2O showed a significantly higher value than anhydrous LiI. The dispersion of Al_2O_3 or SiO_2 enhanced the conductivity further in this system. It was also suggested that the highest conductivity is reached with very fine alumina powder but alumina powders less than some critical radius are less effective.

LiI-Al_2O_3 composite system was investigated using NMR study which showed evidence for occurrence of highly conductive phase. The self-diffusion constant of Li in this system was found to be 8.1×10^{-10} cm^2/sec at 300^{o}K which is 1600 times larger than that in pure LiI matrix. This is a reasonable order of magnitude to explain the enhanced conductivity quantitatively [43]. The effective surface properties of alumina upon the enhancement of conductivity in LiI-Al_2O_3 composite were studied [44] by measuring the thickness of the interface layer. Heat treatment of alumina resulted in a slight decrease of thickness of interfacial layer. The surface properties changed with this treatment. The extent of basic active sites, especially –OH group was found to have an effect on the conductivity enhancement. In their subsequent study [45] they realized further enhancement of conductivity when dispersed with particles of γ- Al_2O_3 whose surface was modified by adsorption of nitrates of alkali and alkaline earths and subsequent thermal decomposition at 800^0C.

Significant enhancement of conductivity was also noticed in other lithium halide dispersed systems that include: LiCl-Al_2O_3 [46], LiBr-H_2O-Al_2O_3(α, β) [47-49] with different dispersoids such as α- Al_2O_3, SiO_2, γ- Al_2O_3, η- Al_2O_3 in LiCl. In the case of η- Al_2O_3(25 m/o) the enhancement was about 2 orders of magnitude measured at 25^0C and the activation energy was found to decrease by half of that for LiCl. Nakamura and Goodenough [47] reported a maximum enhancement of about 2 orders at 43^0C for LiBr.H_2O-Al_2O_3(40 m/o), a maximum of 2 orders of magnitude was also measured by Slade and Thompson [48] who showed that the enhancement was a function of the surface area of alumina particles. In the study of Shiuli and Shahi [49] the maximum enhancement recorded was about 2 orders at 302K for 10 m/o of Al_2O_3. The SEM showed that the distribution of Al_2O_3 was not uniform and the particles of Al_2O_3 of 0.05 μm agglomerated to 0.5 μm.

The occurrence of highly conducting phase found to be present in these systems was studied by Chen Liquan in LiCl; η-Al_2O_3 [46] with mole percent and temperature and Takeshi and Shichio [50] in LiBr-Al_2O_3 from Li NMR spin relaxation times. The amount of this highly conducting phase was found to increase with the amount of dispersed oxide at lower m/o Al_2O_3 and was found to be constant later up to 50 m/o, which means that the thickness of highly conducting phase layer was maintained constant up to 50 m/o of Al_2O_3. This layer was found to decrease linearly with Al_2O_3 content beyond 50 m/o. This explains the composition dependence of enhancement effect.

II.2 FLUORITES

The enhancement of conductivity in fluorides of Ca and Ba was observed by Fujitsu et al. [51] by dispersing with Al_2O_3 particles of sizes 0.3 and 0.06μm. In CaF_2-Al_2O_3 system a maximum enhancement of 1-2 orders of magnitude was observed for 0.06μm at 5 m/o of Al_2O_3 and for 0.3μm at 10m/o of Al_2O_3 at 500°C and it was found to depend on composition as well as particle size of Al_2O_3. A similar variation could be observed in BaF_2 - Al_2O_3 where maximum was observed for 20m/o Al_2O_3 at 500°C for 0.3 and 8μm particles. Explanation for the composition and particle size

dependence of conductivity assumed the formation of highly conductive interface between host matrix and Al_2O_3 particles. The conductivity and the thickness of the interface layer at 500°C were estimated to be 10^{-3} S/cm and 0.3 to 0.6μm respectively by simple mixing model. Addition of Al_2O_3 or ZrO_2 to the polycrystalline CaF_2 [52] was found to increase the conductivity relative to host material. The maximum enhancement was recorded to be 2 orders of magnitude for 10m/o Al_2O_3 powder of the higher surface area from Alcoa Co. and for 5m/o Al_2O_3 samples of lower surface area from Adolf Meller Co. in the low temperature region as well as a decrease in the activation energy for conduction compared to pure CaF_2. The 25m/o composites of both types of alumina showed a decrease in conductivity which was attributed to blocking effects of the insulating Al_2O_3 phase created in the composite.

In ZrO_2 dispersed system a more systematic conductivity behavior was observed where the maximum enhancement occurs at 5m/o in both high and low temperature regions. Increased concentration of fluorine ion interstitials at the interface was thought to be responsible for such enhancement [53]. Measured transport number of fluorine ions in these composites was in support of the above conclusion. The increase in the conductivity was studied in Al_2O_3, CeO_2 dispersed CaF_2 systems by vaidehi et al., [54]. The maximum enhancement observed in Al_2O_3 dispersed system was 2 orders, whereas in CeO_2 dispersed system it was about 3 orders of magnitude at 650° K with respect to pure CaF_2. Buildup of space charge regions at the phase boundaries of dispersed solid electrolyte systems were postulated to cause the enhancement of their ionic conductivities. Some aspects of the increase in the ionic conductivities of this system were explained by Maier's semi-quantitative model based on quasi-parallel switching. The low temperature rise in the conductivity of CaF2 was suggested to be caused by a significant enhancement in the vacancy concentration of CaF2 caused by the attraction of F-ions to the surface of Al2O3 (or CeO2).

The enhancement recorded in fluorite type material $SrCl_2$-Al_2O_3 system [55] was observed to depend on the composition and the grain size of Al_2O_3 and the method of preparation. The particle sizes used in this study were 0.06, 0.3, 1, 3, 8 and 15μm. These Particle sizes were found to aggregate into larger secondary particles during the sample preparation and their average particle sizes were measured to be 2.6, 8.2 and 10μm whose original sizes were 0.3, 3 and 8μm respectively. It was considered that the interface between $SrCl_2$ matrix and Al_2O_3 particles played a major role in giving rise to high ionic conductivity. The conductivity enhancement was estimated to be 2 orders of magnitude while the thickness of the interface layer was estimated by simple mixing model to decrease with increase in temperature from 0.6 to 0.15μm.

In order to evaluate the validity of the estimations made by simple mixing model the conductivity studies on a multi-layered sample were undertaken by the authors (Fujitsu et al.) [55]. This multi-layered sample was prepared by dispersing $SrCl_2$ in sec-butyl alcohol and using this solution to paint both the surfaces of Al_2O_3 as thin plates (50μm.), which were laminated upon each other and finally sandwiched between two thick Al_2O_3 plates. The current was measured parallel to the interface layers. It was observed that the calculated conductivity was slightly higher than the measured conductivity and this was attributed to the imperfect contact between Al_2O_3 plates and $SrCl_2$ layers or due to an experimental error. This experiment leads the authors to believe in the formation of an interfacial layer of sub-micron size between the $SrCl_2$ and Al_2O_3 that produced the enhancement effects.

Two probe ac impedance measurements carried out on PbF_2 when dispersed with CeO_2, SiO_2, ZrO_2 and Al_2O_3 in the frequency range 10 HZ to 10^5 HZ showed an enhancement in the extrinsic conduction [56] region. The adsorption of water was estimated to be 0.1% and 0.2% in Al_2O_3 and SiO_2 respectively when they were exposed to air at room temperature. No new phase was detected by X-Ray powder diffraction in any of the mixtures. The space charge layer that developed at the

oxide/host interface—a result of the chemical events occurring there—was used to explain the conduction mechanism. Particle hydrate comparisons were used to discuss these interactions. A composite made up of particles of a colloidal size distributed throughout an immobilised aqueous solution is called a particle hydrate. This aqueous matrix is immobilised and undergoes proton conduction. With the exception of the salt's crystalline nature, the analogy between an initial pure water aqueous matrix and a colloidal particle scattered throughout a stoichiometric salt is almost precise.

II.3 ALKALINE EARTH NITRATES

Improvement in dc ionic conductivity is observed in the Sr(NO3)2-Al2O3 dispersed solid electrolyte system. was studied by Narender Reddy et al [57-58]. The maximum enhancement of about 3 orders is observed for 29.3m/o of $Sr(NO_3)_2$-Al_2O_3 system. XRD showed no evidence of formation of any solid solution and as per them the very high melting point of the insulator Al_2O_3 also could be a reason why it cannot form a solid solution. Enhancement of conductivity was explained on the basis of the formation of space charge layer. $Sr(NO_3)_2$, being a anti-frenkel type defect solid, enhancement observed in it could be understood as follows: In the space charge area close to the MX/D interface, vacancies of mobile ion species are formed as a result of the interaction between the mobile ions of MX and the dispersoid D. This can occur both when the mobile ions are repelled into the matrix MX to form interstitials and when they are drawn to the phase D, leaving the vacancies at the interface. Of these, it was believed that the production of vacancies was more likely than the formation of interstitials.

They extended their studies on the role of particle size (36.9, 0.3 and 0.06μm) and the dispersoid's mole percentage in $Sr(NO_3)_2$:Al_2O_3 [59] composite solid electrolyte system. The increase in conductivity was found to be dependent on the size of the particle, although for a given particular

surface area, all three particle sizes showed the same gain. In the extrinsic temperature range, an increase in conductivity was observed with a mole percent of the dispersoid. The fall in enhancement at higher mole percent was found to be caused by the dispersoid particles' inclination to cluster together as the total surface area available for interacting with the host material declines.

III THEORETICAL MODELS

A number of phenomenological ideas have been put out in an attempt to explain the mechanism of ion transport in composite electrolyte systems. As of yet, no single cohesive model exists that can explain the wide range of experimental results on distinct composite electrolyte systems in a unique way. The occurrence of a space-charge zone, also referred to as a double layer, at the interface between the host and dispersoid, is the core element of most models proposed to explain conductivity increase in two-phase composite systems. This issue has been the focus of numerous experimental investigations, including the apparent impact of surface hydration [61], the dependency of conductivity on the surface area [60, 61] of alumina, etc.

Furthermore, in certain composite systems, conductivity increases have also been proposed to be caused by bulk interactions [62]. The majority of these models concentrate on calculating the conductivity's compositional dependency. The sole distinctions between them are in the computation techniques and the presumptions made regarding the dispersoid particle distribution within the composite system. We'll talk about a few significant models for composite electrolyte systems below.

III.1 JOW AND WAGNER'S MODEL

In order to characterize the case of space charge regions around spherical inclusions in matrix material of Frenkel type, Kliewer [63] presented the continuum model for the space charge area near surfaces of Frenkel disorder type compounds (like CuCl). Jow and Wagner [61] expanded on Kliewer's idea to explain conductivity increase in a CuCl-Al2O3 composite electrolyte system. They

postulated that the introduction of a dispersoid phase (A) into the electrolyte host matrix (MX) results in the creation of a space charge area at the host and dispersoid interface boundary. The dispersoid particles are surrounded by a λ-thick space charge layer. The cross-sectional image and idealized spherical particle for analytical calculation are shown in Figure III.1. They suggested that the development of oppositely charged defects in the dispersed space charge compensates for the dispersoid particle's charge, though the spin is unknown, at the surface. This leads to the formation of an excess defect concentration in this area. This unanticipated boost was explained by Jow and Wagner as the result of a space charge zone that formed close to the interface between the inert second phase and the matrix electrolyte. The outcome of the second phase's low content's inferred conductivity was displayed as

$$\sigma = \sigma_0 + 3e\mu \langle \Delta n \rangle \lambda (1/r)(P/1-P) \qquad (1)$$

where e is the absolute electronic charge, $\langle \Delta n \rangle$ is the average excess charge density in the space charge, and σ is the bulk ionic conductivity of the matrix material.

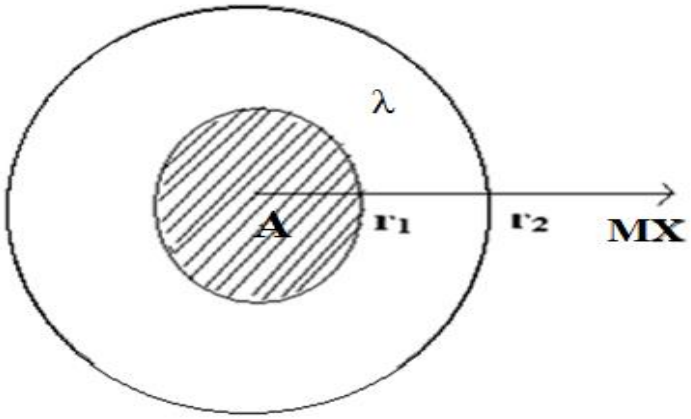

Fig. III.1 An illustration of a single alumina particle in a host matrix in cross-section.

area, λ the Debye length, μ the mobility of the ion or defect species in the matrix material, r the radius of the second phase's dispersoid, and p the second phase's volume content. This model demonstrated

good agreement with the experimental findings at low second phase concentrations. About the assumption's limit, which states that the second phase's size should be substantially smaller than the matrix's. Therefore, the model is unable to explain conductivity maxima observed in several cases for a given mole percentage of the dispersoid.

III.2 MAIER'S MODEL

Maier [64-66] has suggested a method for computing the bulk ionic conductivity in a matrix MX that is ionically conducting and distributed with insulating second phase A. In this it is considered that there is no solubility or chemical reaction except that there is a possibility of surface interaction which is known to occur with oxides between the host matrix MX and insulating phase A. He has also discussed the defect chemistry involved in the space charge region at the interface which is responsible for the conductivity enhancement. The surface interactions at the interface results in the formation of space charge which is exponentially decreases with x (distance) into the interior. The defect reaction at the interface is understood by splitting it into the formation of the bulk vacancies and interstitials in Frenkel type solid.

$$M_M + V_A \leftrightarrow M'_A + V^1_M \qquad (2)$$

$$M'_A + V_1 \leftrightarrow M'_1 + V_A \qquad (3)$$

The first part of the reaction is that when a cation in normal lattice (M_M) goes on to the interface (assuming that there is a vacancy at interface site V_A) and becomes an interfacial cation (M'_A) creating a vacancy in its normal lattice position (V^1_M). In the second part, interface cation (M'_A) will be moved to interstitial position (assuming that there is an interstitial vacancy at V_1), and becomes interstitial cation (M'_1), leaving the interface site vacant again. $\Delta_{VA}G^0$, $\Delta_{IA}G^0$ are the free energies necessary for the vacancy to form and interstitial respectively in the presence of the second phase and

$\Delta_{S1}G^0$ is the energy required for the surface interaction due to phase A's second appearance. The corresponding interaction is given by

$$M_S + V_A \leftrightarrow \quad M'_A + V_S \qquad (4)$$

Where M_S is a surface cation. In this, two cases are possible. One is stabilization of M surface ion by the second phase i.e., an attractive interaction between MX and A-phase. A possible mechanism is shown in Figure III.2(a). If the energy of this mechanism is sufficient enough to compensate the entropic effects, the free energy of the vacancy formation is lowered and that of interstitials is increased compared to the intrinsic values. If $\Delta_{VA}G^0 < \Delta_{IA}G^0$, the surface interaction has the consequence that ions will be sucked out of the volume and the concentration of vacancies will be increased. On the other hand, the M ions will be pushed into interstitial sites (repulsive interaction between A and M_s) as in Figure III.2(b). Thus, an extrinsic conductivity boost is expected in both scenarios for sufficiently strong interactions. This model views each phase as a parallel resistor and treats the space-charge area as a separate phase. The overall conductivity is given by

$$\sigma = \beta_A\varphi_A\sigma_A + \beta_\alpha\varphi_\alpha\sigma_\alpha + \beta_{SC}\varphi_{SC}\sigma_{SC} \qquad (5)$$

Where α denotes the bulk, A denotes the insulating phase and SC space-charge region.The volume proportion of phase A is represented by φA, while β is a quantity that characterizes the departure from optimal parallel switching. The physical situation is shown in figures III.3 (a) and (b).

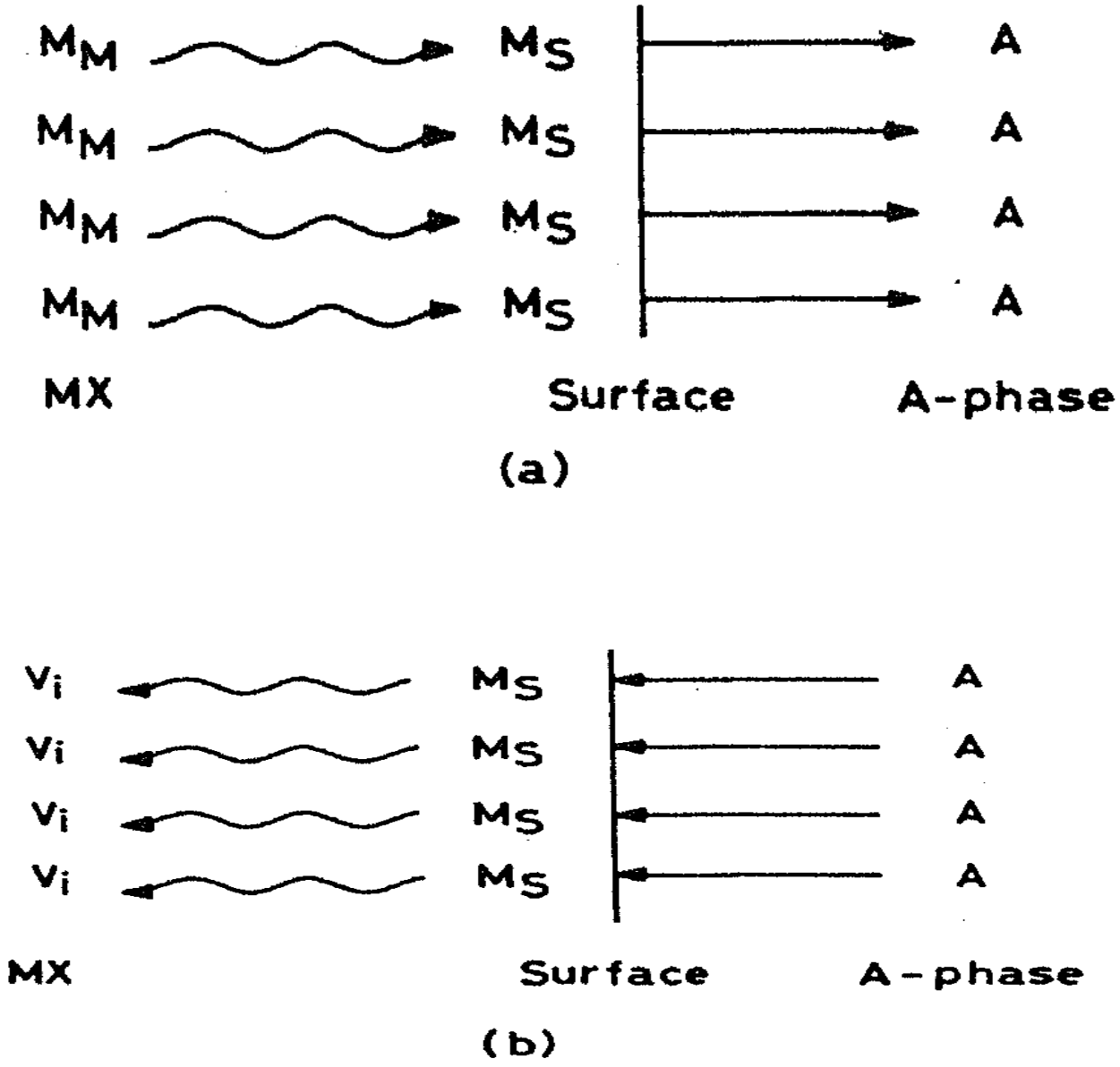

Fig. III.2 The surface effects of a phase on host matrix

(a) An attractive interaction results in enrichment of vacancies.

(b) A repulsive interaction in driving M_S surface ions into interstitial positions.

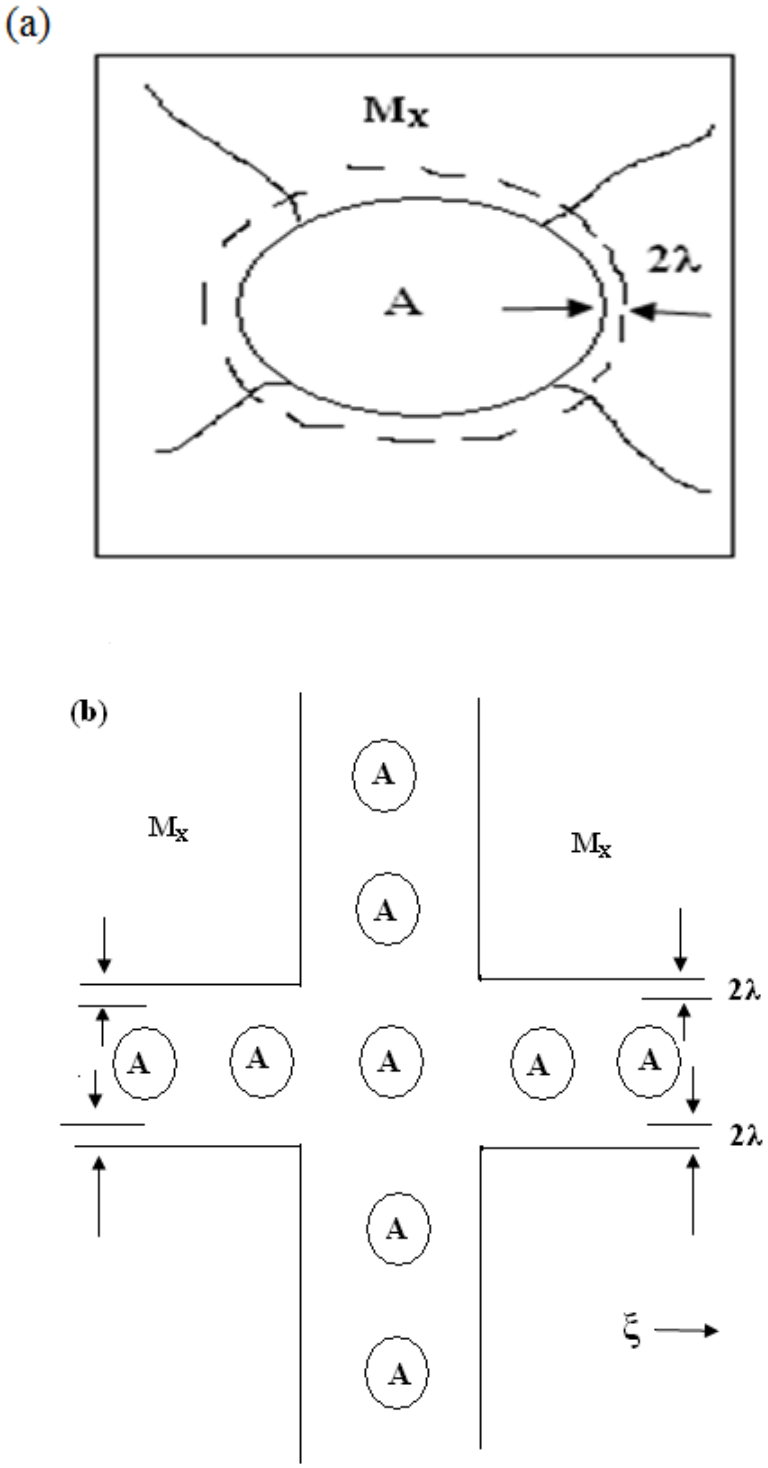

Fig III.3 (a) Phase A particle embedded in MX material and bearing a space charge layer

(b) Coherent Phase A spheres forming crossing chains or areas.

The conductivity component due to the space charge region, from eq.(1) may be written as

$$\sigma_{SC} = e\,(2\lambda)\,\mu_V\,(C_{V0}\,C_{V\alpha})^{1/2} \qquad (6)$$

here, the mobility of vacancies is denoted by μV.The concentrations of vacancies at the bulk and surface are denoted by CVα and CV0, respectively. The space charge layer's effective thickness is two times the proton. It is assumed that the dispersoid particles are spherical and that a space charge zone with a thickness of 2λ encircles them. The space charge layer's volume fraction is found by deducting the inner sphere's volume fraction from the outer sphere's, as shown by

$$\varphi_{SC} = 3\,(2\lambda / r_A)\,\varphi_A \qquad (7)$$

where r_A is radius of the dispersoid particles, so the total conductivity from eqn. (6) is given by

$$\sigma = (1-\varphi_A)\,\sigma_\alpha + 3e^{\beta}_{SC}\,2\lambda\,(\varphi_A / r_A)\,\mu_V\,(C_{V0}\,C_{V\alpha})^{1/2} \qquad (8)$$

It has been observed that the above equation fairly well explains experimental results such as larger conductivity enhancement at low temperatures, particle size dependence, effect of wet dispersoid, etc., for various solid electrolyte systems. This can be achieved by adjusting the ideal parallel switching parameter, βSC, in the range of 0.2-0.7 depending upon distribution topology. Maier's model is appealing because it clarifies the process that leads to surface defect enrichment in the space charge region. While Maier's model effectively explains many of the distinguishing characteristics of composite electrolyte systems, it fell short on a number of points, including the maxima in σ versus φA plots, the assumption of an oversimplified distribution topology that results in quasi-parallel switching and is characterized by a β –factor, and the assumption of spatially constant mobility values., the dielectric constant and the molar volume, neglecting the structural changes, polarization effect , elastic effects etc.

REFERENCES

1) R.W.G. Wyckoff, 'Crystal structures', Interscience pblishers, 2,**(1964)**, 480.
2) R.W.G. Wyckoff, 'Crystal Structures' InterScience Publishers,1,**(1963)**,239.
3) L.Vegard, Z. Phys., 395,**(1922),** 410.
4) R. Birnstock, Z. Krist., 124, **(1967),** 310.
5) A.M. Bon, C. Benoit and O. Bernard, Phys. Stat. Sol.(b), 78, **(1976),**67.
6) R.Srinivasan, Proc. Indian Acad.Sci., 41A, **(1955)**, 49.
7) Sawada, S., Nomura, S. & Fujii, S. (1958). J. Phys. Soc. Jpn, 13, 1549.
8) M K Aydinol, JVMantese and S P Alpay, J. Phys. Condens. Matter, 19, **(2007)**, 210-23.
9) V.M. Patrov, N.I. Giricheva, V.N Petrova and G.V. Girichev Journal of structural chemistry,4,**(1991)**, 494-498.
10) Sawada, S., Nomura, S., Fujii, S., *J. Phys.Soc. Japan*, 13, **(1958),**1549.
11) Sawada, S., Nomura, S., Asao, Y., *J. Phys.Soc. Japan*, 16, **(1961),** 2486.
12) Nolta, J.P., Schubring, N.W., *Phys. Rev.Lett.*, 9, **(1962)**, 285.
13) Nolta, J.P., Schubring, N.W., Dork, R. A., *J.Chem. Phys.*, 42, **(1965)**, 508.
14) M K Aydinol, JVMantese and S P Alpay,, Journal of physics: Condensed matter 19, **(2007),** 496210, (23pp).
15) Neeraj Kumar, , Rabinder Nath, *J. Mater. Environ. Sci.* 2(4), **(2011),** 379-386 ISSN: 2528-2028.
16) H.G. MCADIE, Thermal Analysis (Proc. Of the 3rd ICTA, Davos, 1971), Birkhauser, Basel, 1, **(1972),** 591.
17) A.S. Lidiard, Hdb.Phys.Springer-Verlag, 20, **(1957)**.
18) J.Rolfe, Can.J.Phys.48, **(1964)**,2195.
19) M.M. Nekrasov, B.M. Belyakov and M.K. Rodionov, IZV.VUZ.FIZ (USSR) 4, **(1967),**11.
20) N. Nadler and Rossel, Phys. Stat. Solidi (a), 18, **(1973),** 711.
21) W. Lehfeldt, Z. Physik 85, **(1933),**717.
22) T.E. Phipps and E.G. Patridge, J. Am. Chem. Soc. 51, **(1929),** 1331.
23) H. Kelting and H. Witt, Z. Physik 26, **(1949),**197.
24) J.E. Ambrose and W.E. Wallace, J. Phys. Chem. 63, **(1959),**1536.
25) H. Schultze, Thesis university of Gottingen **(1952)**.
26) Yu. M. Annenkov and V. A. Grishukov, IZV. VUZ. FIZ (USSR), 74, **(1967),**11.
27) J. Arends, H.W. Den Hartog and A.J. Dekker, Phys. Stat. Solidi 10, **(1965),**105.

28) E. K. Zavadowskaya, J.S. Ivankina and I. Ya. Melik Gaikazyan, IZV. VYW. UCHAB, ZAB. FIZ, 12, **(1970),**92.
29) U.V.Subbarao and V.Haribabu, Crystal Lattice defects, 8, **(1978),** 21-26.
30) P. Veeresham, Dr. U. V. Subba Rao, Dr. V. Hari Babu, 18,12, **(1983),**1581-1584.
31) K. Shahi, J.B. Wagner Jr., Journal of physics and chemistry of solids, 43, 8 , **(1982),**713-722.
32) S.L. Garud and K.B. Saraf, Bull Mater. Sci, 31, 4, **(2008),**639-643.
33) C.M. Padma, C.K. Mahadevan, Materials and Manufacturing Processes, 23, 2, **(2008),** 143-150.
34) Jayaram, " Optics and spectroscopy part 1 Tm," Tn Tbs, New Delhi, **(1972)**.
35) J. Kudnovsky, N.E. Christensen, J. Masek, Physical Review B, 43, **(1991),** 15.
36) Wen-Ming Chien, Dhanesh Chandra, Jennifer Franklin, Claudia J. Rawn and Abdel K. Helmy, JCPDS, 48, **(2005)**.
37) Jander, W., Z.Angew. Chem., 42,**(1929)**,462.
38) Wanger,C., J.Phys.Chem.Solids, 33, **(1972)**,1051.
39) Crosbie, G., J Solid state Chem., 25,**(1978)**,367
40) Liang, C.C., J.Electrochem.Soc., 120,**(1973),**1289.
41) Liang, C.C., and Bernette, L.M., J.Electrochem.Soc., 123 no.4, **(1976)**,453-458.
42) S.Pack, Abstract No.133, Electrochemical Society meeting, Los Angels,**(1979)**.
43) Takeshi Asai, Ching-Hsing Hu and Shichio Kawai, mat. Res.Bull.,22,**(1987)**,269-274.
44) Takeshi Asai, Ching-Hsing Hu and Shichio Kawai, Solid State Ionics, 26,**(1988)**,1-4.
45) Takeshi Asai, and Shichio Kawai, Solid State Ionics, 34,**(1989)**, 195-199.
46) Liquan Chen, Zonguan Zhao, Chaoying Wang and Lizirong Kexue Tongbo, 26,**(1981)**,308.
47) Nakamura,O.and Goodenough,J.B., Solid State Ionics, 7,**(1982)**,125-128.
48) Slade,C.T. and Thompson, M.,Solid State Ionics, 26,**(1988)**,287-294.
49) Shiuli Gupta, patnaik, S., Chaklanobis, S. Chaklanobis, S. and Shahi,K., Solid state Ionics,31,**(1988)**,5-8.
50) Takeshi Asai and Shichio Kawai, Solid State Ionics, 20,**(1986)**,225-229.
51) Fujitsu,S., Miyayama,M., Koumoto,K. and Yanagida,H., J.Mat.Sci., 20,**(1985)**,2103-2109.
52) Kandkar,A., Tare,V.B. and Wagner,J.B., Revue de Chemie Minerale, t.23,**(1986)**,274.
53) Wen,T.L., Huggins,R.A., Rabenau,A. and Weppner, W., Revue de Chimie Minerale, 20,**(1983)**,643.
54) Vaideshi,N., Akila, R., Shukla,A.K. and Jacob,K.T., Mat.Res.Bull., 21,**(1986)**,909.
55) Fujitsu,S., Koumoto,K. and Yanagida,H., SolidState Ionics, 18 and 19,**(1986)**,1146-1149.
56) Shukla,A.K., ManoharanR. And Goodenough,J.B., SolidState Ionics,26,**(1988)**,5-10.

57) S.Narender Reddy, A.Sadananda Chary and T.Chiranjivi, Solid State Ionics 34,**(1989)**,73-77.

58) S.N.Reddy, and A.S.Chary and T.Chiranjivi, J. of Materials sci-Mat. In Electronois.

59) S.Narender Reddy, A.S.Chary and T.Chiranjivi, Solid State Ionics, 66,**(1993)**,131.

60) shahi,k. and wagner, J.B., J.Solid State Chem.41,**(1982)**,107.

61) Jow and Wagner, J.B., J.Electrochem.Soc. 126,**(1979)**,163.

62) Chowdary,P., Tare,V.B. and Wagner J.B., J.Electrochem.Soc.,**(1985)**,123-124.

63) K.L.Kliewer, J.Phys.Chem.Solids, 27,**(1966)**,705.

64) Maier,J., Phys.Stat.Sol(b), 123,**(1984),**K89.

65) Maier,J., J.Mat.Res.Bull., 20,**(1985)**,383-392.

66) Maier,J., Prog.Solid.State Chem., 23,**(1995)**.